ACCEPTED TO THE ASTROPHYSICAL JOURNAL
Preprint typeset using LaTeX style emulateapj v. 8/13/10

THE INTERIOR STRUCTURE CONSTANTS AS AN AGE DIAGNOSTIC FOR LOW-MASS, PRE-MAIN SEQUENCE DETACHED ECLIPSING BINARY STARS

GREGORY A. FEIDEN
Department of Physics and Astronomy, Dartmouth College, 6127 Wilder Laboratory,
Hanover, NH 03755, USA; Gregory.A.Feiden.GR@Dartmouth.edu

AARON DOTTER
Research School of Astronomy and Astrophysics, The Australian National University,
Weston, ACT 2611, Australia; aaron.dotter@gmail.com
Accepted to the Astrophysical Journal

ABSTRACT

We propose a novel method for determining the ages of low-mass, pre-main sequence stellar systems using the apsidal motion of low-mass detached eclipsing binaries. The apsidal motion of a binary system with an eccentric orbit provides information regarding the interior structure constants of the individual stars. These constants are related to the normalized stellar interior density distribution and can be extracted from the predictions of stellar evolution models. We demonstrate that low-mass, pre-main sequence stars undergoing radiative core contraction display rapidly changing interior structure constants (greater than 5% per 10 Myr) that, when combined with observational determinations of the interior structure constants (with 5 – 10% precision), allow for a robust age estimate. This age estimate, unlike those based on surface quantities, is largely insensitive to the surface layer where effects of magnetic activity are likely to be most pronounced. On the main sequence, where age sensitivity is minimal, the interior structure constants provide a valuable test of the physics used in stellar structure models of low-mass stars. There are currently no known systems where this technique is applicable. Nevertheless, the emphasis on time domain astronomy with current missions, such as *Kepler*, and future missions, such as LSST, has the potential to discover systems where the proposed method will be observationally feasible.

Subject headings: binaries: eclipsing — stars: evolution — stars: low-mass

1. INTRODUCTION

In the study of the structure and evolution of low-mass stars, there are a variety of different methods capable of yielding reasonably accurate age estimates; for a thorough discussion of the different methods, and their strengths and weaknesses, see the review by Soderblom (2010). One such method uses detached eclipsing binaries (DEBs) to assign an age. DEBs are fantastic systems for studying stellar evolution. Observations can provide precise masses and radii for the component stars that are nearly model independent (see reviews by Andersen 1991; Torres et al. 2010). Tight constraints on the stellar masses and radii allow for stringent tests of stellar evolution models. Furthermore, the age of a DEB system can be derived if stellar models can predict the radius of each star in the binary at a common age and with a single chemical composition.

Deriving an age estimate from a DEB is straightforward once precise masses and radii are extracted from the data. However, the reliability of the age estimate is contingent upon the accuracy of the stellar models. Recently, pre-main sequence (pre-MS) and MS models of low-mass stars ($< 0.8 M_{\odot}$) have received substantial criticism for not accurately predicting the radii of stars in DEBs. As the number of DEBs with precisely measured masses and radii has increased, it has become clear that stellar models under-predict the radii of stars in DEBs by upward of 10% (see, for example, Mathieu et al. 2007; Jackson et al. 2009; Torres et al. 2010; Feiden & Chaboyer 2012a). The discrepancies between model and observed radii have been largely attributed to the effects of magnetic fields and magnetic activity (Ribas 2006; Chabrier et al. 2007; Jackson et al. 2009; Morales et al. 2010). When present, the discrepancy between observations and model predictions severely limits the use of stellar evolution models to derive the age of individual DEB systems.

We propose a novel method to use low-mass, pre-MS DEBs to estimate the ages of young stellar systems. Instead of comparing individual stellar surface properties to stellar evolution models, we propose to use the dynamics of the DEB system. That is, comparing the observed rate of apsidal motion to stellar model predictions computed using the interior structure constants. This technique is less sensitive to the surface effects of magnetic fields than are methods that only invoke the stellar radius or effective temperature. Our method has the potential to provide a more reliable age estimate.

Below, we outline the model calculations (Section 2), including the computation of the interior structure constants (Section 3). Results pertaining to the time evolution of the interior structure constants as a function of stellar mass are given in Section 4. We conclude with a discussion of the usefulness of this method in Section 5.

2. MODELS

2.1. *Microphysics*

Model evolutionary tracks used in this study were computed with the Dartmouth Stellar Evolution Program (DSEP).[1] The physics incorporated in the models have been described extensively in the literature (Chaboyer & Kim 1995; Chaboyer et al. 2001; Bjork & Chaboyer 2006;

[1] Available at http://stellar.dartmouth.edu/models/

Dotter et al. 2007, 2008; Feiden et al. 2011), but we will provide a brief overview of the physics pertinent to the present study.

Arguably the most critical component of low-mass stellar evolution models is the equation of state (EOS). For masses considered in this study DSEP uses the FreeEOS[2] in the EOS4 configuration. We selected the FreeEOS for three primary reasons. First, it includes non-ideal contributions to the EOS, such as Coulomb interactions and pressure ionization, that become important in the dense plasma of low-mass stars. Second, the FreeEOS calculates the EOS for hydrogen, helium, and eighteen heavier elements as opposed to only calculating the EOS for hydrogen and helium. Finally, the FreeEOS may be called directly from within the stellar evolution code. This feature avoids the need to interpolate within EOS tables, thereby minimizing numerical errors.

Conditions near the outer, optically thin layers of low-mass stars preclude the use of gray atmosphere approximations (Chabrier & Baraffe 2000, and references therein). Therefore, we use the PHOENIX AMES-COND model atmospheres (Hauschildt et al. 1999a,b) to define the surface boundary conditions for our interior models. The atmosphere models are attached at the photosphere,[3] taken to be the point where $T = T_{\rm eff}$.

The radiative opacities we adopt are the OPAL opacities above 10^4 K (Iglesias & Rogers 1996) in combination with the Ferguson et al. (2005) opacities below 10^4 K. For models that are not fully-convective, helium and heavy element diffusion are treated according to the formulation of Thoul et al. (1994). Fully-convective models are assumed to be completely and homogeneously mixed because the convective timescale is considerably faster than the diffusion timescale (Michaud et al. 1984).

2.2. *Solar Calibration*

The primary input variables of stellar evolution models are defined relative to the Sun. These input variables include the stellar mass, the initial mass fractions of helium (Y_i) and heavy elements (Z_i), and the convective mixing-length ($\alpha_{\rm MLT}$). Therefore, we must first define what constitutes the Sun for our model setup. We require that a 1 $M_\odot$ model accurately predict the solar radius, the solar luminosity, the radius to the base of the solar convection zone, and the solar photospheric (Z/X) at the solar age (4.57 Gyr; Bahcall et al. 2005) By iterating over different combinations of Y_i, Z_i, and $\alpha_{\rm MLT}$ we are able to converge upon a solution for the Sun. The final set of variables that satisfies the above criteria for the solar heavy element composition of Grevesse & Sauval (1998) was $Y_i = 0.27491$, $Z_i = 0.01884$, and $\alpha_{\rm MLT} = 1.938$.

3. INTERIOR STRUCTURE CONSTANTS

The distribution of mass within a star in a close binary system is influenced by the star's rotation and by tidal interaction with its companion. Imagine two stars, A and B. The rotation of star A and the tidal interaction of star B with star A distorts the shape of star A. Instead of remaining spherically symmetric, the equilibrium configuration of star A will become ellipsoidal. Subsequently, the gravitational potential of star A will also become ellipsoidal. The same can be said from the perspective of star B.

If the binary orbit is elliptical, the distorted gravitational potential will cause the orbit to precess. This precession may be likened to the precession of Mercury's orbit about the Sun—although, Mercury's precession is due to general relativity. The precession of the binary orbit is known as apsidal motion.

The rate of apsidal motion ($\dot{\omega}$; measured in degrees per cycle), or the rate at which the orbit precesses, is governed by the shape of the gravitational potential, which may be deformed as discussed above. Therefore, $\dot{\omega}$ depends on the properties of the stars and of the orbit. Explicitly,

$$\dot{\omega} = \left(\frac{c_{2,1} + c_{2,2}}{360} \right) \overline{k_2}, \tag{1}$$

where

$$c_{2,i} = \left[\left(\frac{\Omega_i}{\Omega_K} \right)^2 \left(1 + \frac{m_{3-i}}{m_i} \right) f(e) + \frac{15 m_{3-i}}{m_i} g(e) \right] \left(\frac{R_i}{A} \right)^5. \tag{2}$$

In the above equation, Ω_K is the mean orbital angular velocity, Ω_i, m_i, and R_i are the rotational velocity, the mass, and the radius of the i-th component in the binary, respectively. Additionally, A is the semi-major axis of the orbit,

$$f(e) = (1 - e^2)^{-2}, \tag{3}$$

and

$$g(e) = \frac{(8 + 12e^2 + e^4)}{8} f(e)^{5/2}, \tag{4}$$

with e being the eccentricity of the orbit. Finally, the last term in Equation (1), $\overline{k_2}$, is the weighted interior structure constant observed for the two binary stars. In general,

$$\overline{k_2} = \frac{c_{2,1} k_{2,1} + c_{2,2} k_{2,2}}{c_{2,1} + c_{2,2}}. \tag{5}$$

Here, $k_{2,1}$ and $k_{2,2}$ are the interior structure constants for each star.

Equations (1)–(5) are derived from a j-th order solid harmonic expansion of the gravitational potential (see, for example, Kopal 1978). The interior structure constant for a given star, k_2, is the second-order term from a more general set of expansion coefficients, k_j. These second-order coefficients quantify the central concentration—or distribution—of mass within a star (Kopal 1978). Lower values of k_2 correspond to a higher level of central mass concentration. Point sources, for example, have $k_2 = 0$.

Observationally, we can not solve for the individual $k_{2,i}$ values. However, in the above equations, every variable is a direct observable, except for $\overline{k_2}$. The latter must be inferred from observational determinations of $\dot{\omega}$ and the $c_{2,i}$ coefficients. Since the individual $k_{2,i}$ values depend on the stellar density distribution, they can provide deep insight into the validity of stellar evolution models. To bypass the restriction that only $\overline{k_2}$ can be inferred from observations, we use k_2 values from stellar evolution models in combination with the observed $c_{2,i}$ coefficients to derive a theoretical $\overline{k_2}$.

DSEP is equipped to calculate the general interior structure constants, k_j, for a star at every evolutionary time step. This is achieved by solving Radau's equation after each model it-

[2] By Alan Irwin: http://freeeos.sourceforge.net

[3] The choice of where to attach the model atmosphere to the interior model is an important one. Our experience indicates that attaching the atmosphere at $T = T_{\rm eff}$ is reasonable for $M \gtrsim 0.2 M_\odot$; for lower masses it is necessary to attach the model atmosphere deeper into the interior.

eration. Following the formalism outlined by Kopal (1978),

$$a\frac{d\eta_j}{da}+\frac{6\rho(a)}{\langle\rho\rangle}(\eta_j+1)+\eta_j(\eta_j-1)=j(j+1) \quad (6)$$

with $j\in\{2,3,4,\ldots\}$ being the order of the solid harmonic, a is the radius of an equipotential surface ($a=r$ when the surfaces are spherically symmetric), and

$$\eta_j(a)=\frac{a}{\varepsilon_j}\frac{d\varepsilon_j}{da}. \quad (7)$$

In the above equation, ε_j is the stellar deviation from sphericity. We also introduced $\rho(a)$, the density of the stellar plasma at radius a, and $\langle\rho\rangle$, the volume averaged density at each radius,

$$\langle\rho\rangle=\frac{3}{a^3}\int_0^a\rho(a')a'^2da'. \quad (8)$$

If we assume that tides and rotation do not significantly alter the shape of a star, we are permitted to use a spherically symmetric model to compute the interior structure constant. Our code employs a 4th-order Runge-Kutta integration scheme to obtain a particular solution of Radau's equation at the stellar photosphere. Interior structure constants are then directly related to the particular solutions at the surface, $\eta_j(R)$, through

$$k_j=\frac{j+1-\eta_j(R)}{2\,[j+\eta_j(R)]}. \quad (9)$$

But, is it reasonable to assume that the stellar mass is not significantly redistributed due to rotation and tides?

The effect of rotation on the central mass concentration of stars with a total mass greater than $0.8\,M_\odot$ was investigated in several previous studies (Stothers 1974; Claret & Giménez 1993; Claret 1999). For stars less massive than $0.8\,M_\odot$, the effect of rotation should be negligible because they have a higher mean density compared to solar-type stars. To test this assumption, we used Chandrasekhar's analysis of slowly rotating polytropes to estimate the amount of oblateness—or deviation from spherical symmetry—rotating low-mass stars may be expected to have.

Chandrasekhar (1933) derived an analytical expression for the stellar oblateness for slowly rotating polytropes. The oblateness was defined to be the relative difference between the equatorial radius and the polar radius,

$$\mathcal{F}\equiv\frac{r_{\rm eq}-r_{\rm pole}}{r_{\rm eq}}, \quad (10)$$

with $r_{\rm eq}$ and $r_{\rm pole}$ being the equatorial and polar radius, respectively. Polytropes were considered slowly rotating when

$$\chi\equiv\frac{\Omega^2}{2\pi G\rho_c}\ll 1, \quad (11)$$

where Ω is the stellar angular velocity, G is the gravitational constant, and ρ_c is the mass density in the stellar core. Does this criterion apply to real low-mass stars? If we assume a rotation period of 1.0 day and a core density of 10 g cm^{-3} (realistic for pre-MS low-mass stars), then $\chi\approx 10^{-3}$.

The result of Chandrasekhar's analysis was a relation between the stellar oblateness and χ for different values of the polytropic index, n,

$$\mathcal{F}=\begin{cases}5.79\chi & \text{for } n=1.5\\ 9.82\chi & \text{for } n=2.0\\ 41.8\chi & \text{for } n=3.0\end{cases}. \quad (12)$$

Stars with masses below $0.65\,M_\odot$ are best represented by a polytrope with $1.5<n<2.0$. Assuming $n=2.0$, a low-mass star will have $\mathcal{F}\sim 0.01$. This treatment indicates that the effect of rotation on the sphericity of low-mass stars is a 1% effect; rotation will not be addressed in this study.

Assessing the influence of tides is difficult. We expect spherically symmetric models to provide accurate estimates of the mass distribution if $R_*\ll R_{\rm roche}$, where $R_{\rm roche}$ is the Roche lobe radius.

We also caution that the configuration of the binary must be considered. If the rotational axes are not aligned, as found with DI Her (Albrecht et al. 2009), then the validity of the assumptions required to derive of k_2 no longer hold. See Section 5 for a further discussion.

General relativistic distortion of the gravitational potential also plays a role in determining the rate of apsidal motion (Giménez 1985). This contribution to the apsidal motion rate can be added to the classical contribution (i.e., Equation (1))

$$\dot\omega_{\rm tot}=\dot\omega_N+\dot\omega_{\rm GR}, \quad (13)$$

where $\dot\omega_{\rm tot}$, $\dot\omega_N$, and $\dot\omega_{\rm GR}$ are the total apsidal motion rate, classical apsidal motion rate, and the rate predicted from general relativity. The general relativistic contribution does not depend on the mass distribution of the stars. Thus, general relativity does not affect the theoretical derivation of the interior structure constants, but must be accounted for prior to comparing the theoretical and observational determinations of $\overline{k_2}$.

4. RESULTS

4.1. *Single Stars*

Individual, solar-metallicity evolutionary tracks were computed for several masses ranging from the fully-convective regime ($0.25\,M_\odot$) up to masses where stars have thin convective envelopes ($0.75\,M_\odot$). Near the boundary where the transition from a radiative core to a fully-convective interior is expected ($\sim 0.35\,M_\odot$), a finer grid of mass tracks was generated to allow for further exploration. The evolution of k_2 with age for each mass track is presented in Figure 1. The full collection of mass tracks used hereafter have been made available on the Dartmouth Stellar Evolution Database[4].

Stellar models that develop a radiative core have a rapidly-changing interior structure constant between the age of 10 and 100 Myr. This can be observed in Figure 1(a). As the convection zone recedes, the central regions of the collapsing pre-MS star create a more centrally-concentrated mass profile, lowering the derived value of k_2. The result is that the value of k_2 decreases by about 5% – 10% every 10 Myr for masses above $0.45\,M_\odot$. Masses below approximately $0.45\,M_\odot$ undergo variations up to about 5%.

This period of rapid contraction continues until a small convective core develops, producing a star with three energy transfer zones: a convective core, a radiative shell, and a convective outer envelope. The star settles onto the MS once the small convective core subsides with the equilibration of ^{3}He burning. In Figure 1, this process is manifested by the upward turn of the mass tracks near 100 Myr, followed by a flattening of k_2 as the star enters the MS.

After first developing a small radiative core on the pre-MS, stars with masses between $0.29\,M_\odot$ and $0.35\,M_\odot$ eventually maintain a fully-convective interior (see Figure 1(b)). These

[4] http://stellar.dartmouth.edu/models/k2.html

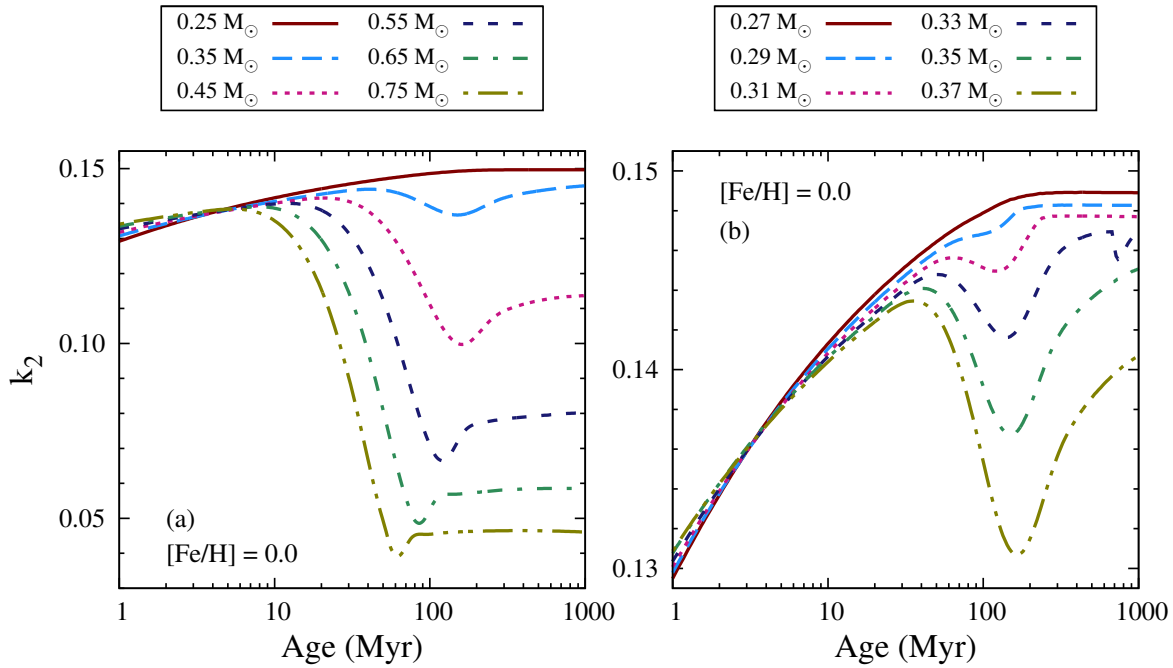

Figure 1. The time evolution of the interior structure constant, k_2, for stars of various masses. Stars that develop a radiative core during the pre-main sequence exhibit rapidly decreasing k_2 values between roughly 10 and 100 Myr. (a) Total range of masses considered in this study shown in increments of 0.05 $M_\odot$. (b) A detailed view of the transition to fully-convective interiors. Only the 0.37 $M_\odot$ model does not ultimately become fully-convective.

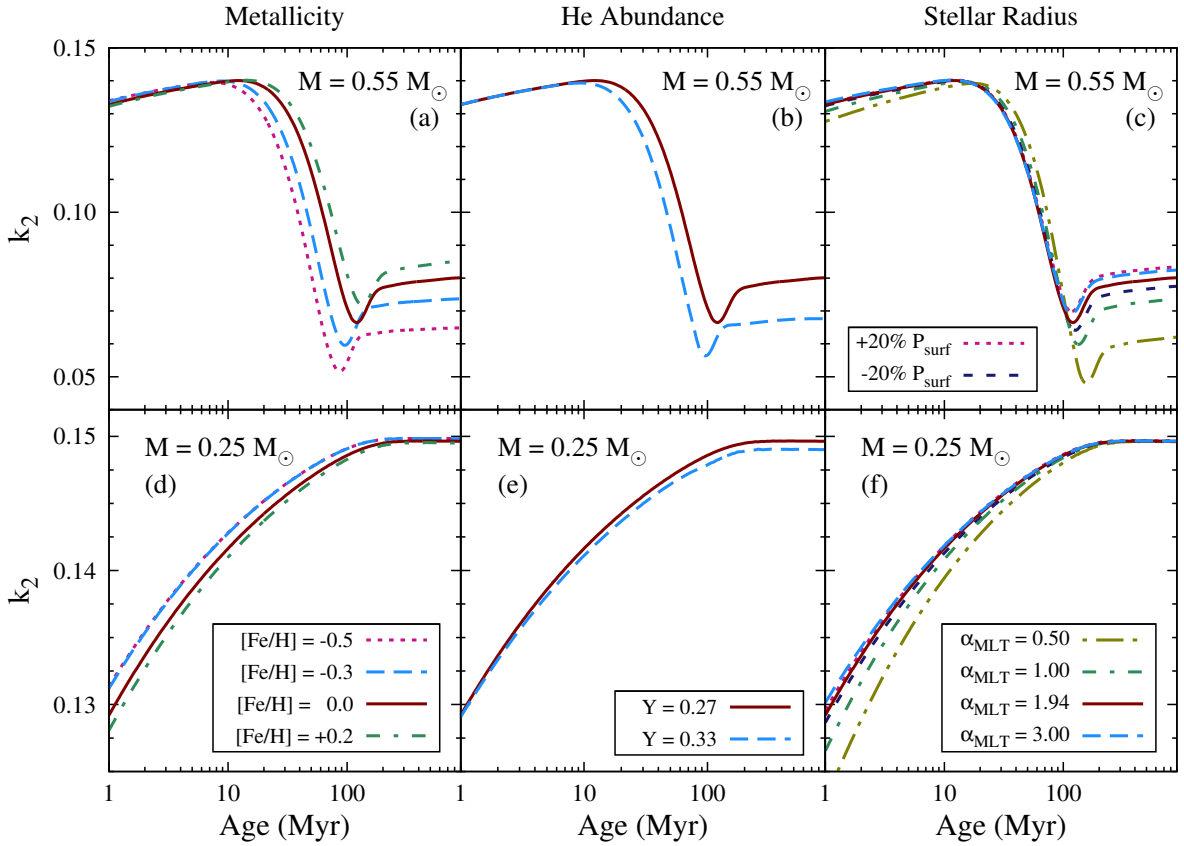

Figure 2. The influence of various model properties on the predicted evolution of k_2 for two different stellar masses. From left to right, the properties investigated are: scaled-solar metallicity in (a) and (d), helium mass fraction (Y) in (b) and (e), and artificial radius changes in (c) and (f). Models in the top panels ((a)–(c)) show a 0.55 $M_\odot$ star while the bottom series ((d)–(f)) show a fully-convective 0.25 $M_\odot$ star. Note, the legend for panels (c) and (f) is split between the top and bottom panels due to space restrictions. The separate tracks indicated by both legends are presented for each mass.

small radiative cores manifest themselves as small dips in the evolution of k_2, just as for stars that maintain a radiative core on the MS. While the rate of change in k_2 is rapid during the core contraction, the relative change in k_2 with stellar age is small ($< 5\%$). It is evident from Figure 1(b) that near the fully-convective transition, stars that eventually end up with fully-convective interiors exhibit a degeneracy in the age-k_2 plane. There is no differentiating between their pre-MS core contraction and the eventual reduction of the radiative shell using k_2 alone. Below 0.29 $M_\odot$, a radiative core does not develop on the pre-MS.

Additional models were generated to investigate the effect of specific stellar properties on the predicted values of k_2. In Figures 2(a)–(f) we illustrate the results of changing the scaled-solar stellar metallicity, helium abundance (Y), and the effects of artificially inflating and deflating the stellar radius. For this exercise, two masses were selected to study the effects on the two broad categories of low-mass stars: fully-convective stars and stars with radiative cores.

It is apparent from Figure 2 that changes to the chemical composition have the largest effect on the value of the interior structure constant on the pre-MS. Variations in metallicity of 0.2 dex translate into a 5% difference in the calculated k_2 for a 0.55 $M_\odot$ star at a given pre-MS age. Similarly, large variations in the helium abundance have the ability to produce changes in k_2 at the 5% level.

Without some prior knowledge of the stellar composition, the effects of such variations may be confused with a difference in stellar age. The effects on k_2 are lessened as mass decreases, until variations nearly vanish in the fully-convective regime (panels (d) and (e) of Figure 2). Note that a change in Y pushes k_2 in the same direction in both mass regimes, whereas a change in metallicity produces a change in one direction for the radiative core case but the opposite direction in the fully-convective case. While this behavior does not lift the age-composition degeneracy entirely, it could prove a useful diagnostic in DEB systems whose components straddle the fully-convective boundary.

We attempted to mimic the possible effects of magnetic fields on the structure of our models by computing models at solar-metallicity with $\alpha_{\rm MLT}$ = 0.5, 1, and 3. The modified mixing-length represents magnetic suppression of convection in the deep interior. Additionally, models were run where we artificially changed the surface pressure by $\pm$20%. The altered surface pressure represents the possible influence of star spots on the stellar photosphere. The magnetic Dartmouth models (Feiden & Chaboyer 2012b) were not used as they have yet to be evaluated for stars on the pre-MS.

Figures 2(c) and 2(f) show how k_2 varies with changes to $\alpha_{\rm MLT}$ and the surface pressure. During the pre-MS contraction, a 20% change in the surface pressure results in a $\sim 2\%$ change to the stellar radius. The accompanying change in k_2 was found to be 0.2% and 1.0%, for a positive and negative change to the surface pressure, respectively. In the 0.55 $M_\odot$ models, increasing $\alpha_{\rm MLT}$ to 3 yielded a stellar radius that was 2% smaller than our solar-calibrated model with k_2 variations under 1% throughout the star's pre-MS contraction. Decreasing $\alpha_{\rm MLT}$, however, produced larger variations in k_2. At an age of 60 Myr the model radii appeared inflated by 5% and 15% for $\alpha_{\rm MLT}$ = 1.0 and 0.5, respectively. The corresponding changes in k_2 were, respectively, 4% and 12%. Panel (f) of Figure 2 indicates that the 0.25 $M_\odot$, fully-convective models experience the greatest differences at the youngest age and that these differences diminish until the different tracks converge on the MS. These changes to $\alpha_{\rm MLT}$ and surface pressure are for illustrative purposes only. It is not at all clear that simply reducing $\alpha_{\rm MLT}$ is a suitable approximation for the presence of an interior magnetic field nor that altering the surface pressure is a good approximation for star spots at the surface.

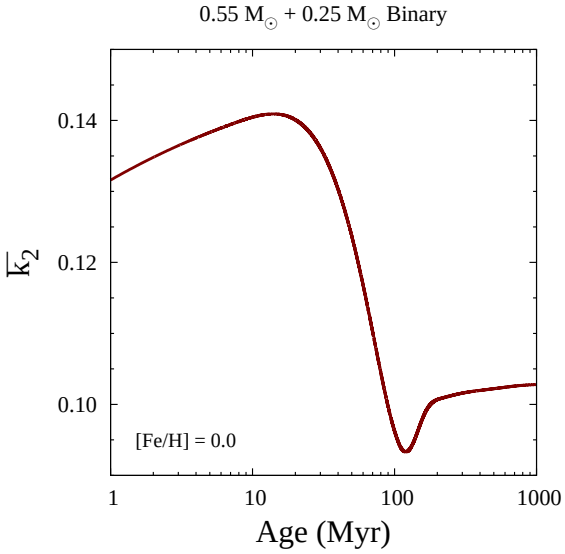

Figure 3. The evolution of the theoretical $\overline{k_2}$ for a binary having a $0.55M_\odot$ primary and a $0.25M_\odot$ secondary. The "observed" stellar radii are fixed at $0.62R_\odot$ and $0.41R_\odot$ for the primary and secondary, respectively (see Section 4.2). The orbit was chosen to have an eccentricity $e = 0.2$.

4.2. *Binary Systems*

The rapid evolution of k_2 for a single star can provide an accurate age estimate for that star, but what about for a binary system? We stated in Section 3 that observations are only able to provide the weighted mean value of k_2 for two stars in a binary. To derive an age estimate for a binary system, we must find the theoretical $\overline{k_2}$.

Temporal evolution of the theoretical $\overline{k_2}$ values can be obtained by combining two k_2 mass tracks using Equation (5). Computation of the $c_{2,i}$ coefficients requires precise knowledge of the stellar masses, radii, and the orbital eccentricity (see Equation (2) and note that A becomes irrelevant). The angular velocity term in Equation (2) can either be measured or approximated using the orbital eccentricity, assuming pseudo-synchronization (Kopal 1978),

$$\Omega_i^2 = \frac{(1+e)}{(1-e)^3}\Omega_K^2. \tag{14}$$

Hence our reason for focusing on DEBs: they can yield precise estimates of the stellar and orbital properties.

The evolution of $\overline{k_2}$ is simplest for an equal mass binary. In this case, both stars contribute equally to $\overline{k_2}$, meaning the $\overline{k_2}$ track is exactly equal to the two individual k_2 tracks. The discussion from Section 4.1 on single star tracks would then apply to the binary system.

A binary with unequal mass components is not so simple. Two mass tracks are required—one computed for the mass of each star—and must be combined as a single track using Equation (5). How does this effect our ability to extract an age estimate?

We have provided an example of a weighted k_2 evolutionary track in Figure 3. The masses selected are those of the two stars presented in Figure 2, $M_1 = 0.55M_\odot$ and $M_2 = 0.25M_\odot$.

For this example, we arbitrarily adopted an orbit with an eccentricity $e = 0.2$. Weighting of the theoretical k_2 values is insensitive to the semi-major axis. The stellar radii ($R_1 = 0.62R_\odot$ and $R_2 = 0.41R_\odot$) were selected from a solar metallicity mass track at an age of 40 Myr. To simulate the type of data available to an observer, we elected to fix the radius, and thus, fix the $c_{2,i}$ coefficients (used to weight the value of k_2) at each age in Figure 3.

The rapid evolution of k_2 that is taking place in the $0.55M_\odot$ star largely dominates the relatively slow k_2 evolution of the $0.25M_\odot$ star. While the weighted k_2 value for the binary does not evolve as rapidly as for a single $0.55M_\odot$ star, the weighted value still changes by about 5% every 10 Myr. This is comparable to models of single stars and should not significantly hinder any age analysis.

5. DISCUSSION

DEBs provide an excellent laboratory for testing stellar structure and evolution theory in different mass and evolutionary regimes. The mass-radius plane is the strictest test of stellar models because these two quantities are best constrained by the observations (Torres et al. 2010). Results from studies performing such comparisons have led to the consensus that standard stellar evolution models are unable to accurately reproduce the observed stellar radii for masses below $\sim 0.8M_\odot$ (e.g., Torres et al. 2010; Feiden & Chaboyer 2012a). The model inaccuracies are particularly evident among pre-MS binaries (Mathieu et al. 2007; Jackson et al. 2009).

Radius discrepancies of approximately 10 – 15% are routinely quoted between pre-MS DEBs and models. This makes it difficult to derive an age with less than 50% uncertainty from stellar positions in the mass-radius plane. Magnetic effects, particularly surface spots, are thought to belie the observed radius deviations. Canonical stellar evolution models are non-magnetic and are therefore unable to properly account for magnetic modifications to convective energy transport and for the presence of magnetic spots on the stellar photosphere.

We therefore advocate the inclusion of the interior structure constant, $\overline{k_2}$, to overcome these age determination inaccuracies whenever possible. While this study does not lead to us to conclude that individual k_2 values (and thus $\overline{k_2}$) are entirely insensitive to magnetic activity in low-mass stars, it is evident that $\overline{k_2}$ has the potential to be a better diagnostic of the pre-MS evolutionary state than the stellar radius when surface magnetic activity is present.

For instance, setting $\alpha_{\rm MLT} = 0.5$ increases the radius and k_2 of a single star by 15% and 12%, respectively. Fixing the radius to determine an age leads to an age that is upward of 180% greater than if we assume a solar calibrated $\alpha_{\rm MLT}$. On the other hand, fixing k_2 leads to only a 20% greater age. The age errors are then compounded when we consider both stars in the binary. The decreased sensitivity of the individual k_2 values makes the mean $\overline{k_2}$ a superior choice compared to surface quantities like the radius and effective temperature.

The age precision returned from observational determinations of $\overline{k_2}$ is dependent on the precision with which the observational $\overline{k_2}$ and the system's metallicity are known. For example, given an equal mass binary with $0.5\,M_\odot$ stars, knowing $\overline{k_2}$ with 5% uncertainty and the metallicity to ± 0.2 dex yields a pre-MS age with an uncertainty of approximately 33%. Constraining the metallicity uncertainty to ± 0.1 dex improves this age uncertainty to 20%. Furthermore, to obtain an age with 5% precision would require $\overline{k_2}$ to be measured with near 1% precision for a metallicity known to within 0.1 dex.

5.1. *Observational Considerations*

The results presented and discussed above show that it is possible to precisely derive the age of a binary system from measurements of apsidal motion. However, obtaining precise observations of apsidal motion and measuring $\overline{k_2}$ with 5% precision is a painstaking task. The binary system must meet several criteria and the data must be of high quality.

Foremost is that the binary *must* be a double-lined, eclipsing system. While this has been alluded to, we have yet to illuminate precisely why this is so. The reason for requiring a DEB stems from the need for extremely accurate and precise stellar and orbital properties. Equations (1) and (2) reveal that derivation of $\overline{k_2}$ requires exquisite knowledge of the stellar mass ratio, the stellar radii, and the orbital properties (eccentricity and semi-major axis). Only data from DEBs can provide these quantities in a (nearly) model-independent fashion (Andersen 1991; Torres et al. 2010).

A meticulous examination of the binary light curve and radial velocity curve is of the utmost importance. The light curve must be assembled from multi-epoch, time-series differential photometry and must provide nearly complete phase coverage. This latter feature is essential. Not only must the primary and secondary eclipses be captured, but also the behavior of the light curve out of eclipse. Such data is becoming increasingly available with the latest generation of photometric surveys (e.g., *Kepler*, CoRoT[5], SuperWASP[6]) and those to come (e.g., LSST[7], BRITE[8] Constellation Mission).

Similar to the photometry, a large number of high dispersion, high signal-to-noise spectra are needed to construct a detailed radial velocity curve. Attempts must be made to provide adequate phase coverage (see Andersen 1991) and uncover deviations due to the Rossiter-McLaughlin effect (Rossiter 1924; McLaughlin 1924) for reasons we shall discuss momentarily. Torres (2012) points out that the spectroscopy is still the limiting factor of quality in DEB analyses.

Only with the quality of data described above and within Andersen (1991) and Torres et al. (2010) can a truly adequate analysis of a DEB be performed. However, acquisition of data of such quality is very rewarding and allows for a rigorous examination and characterization of the stellar system. It would permit the measurement of the stellar masses and radii with extreme precision (below 2%). This is imperative considering that Equation (2) depends upon the fractional radii (R/A) to the $5^{\rm th}$ power. Additionally, actual measurement of $\dot{\omega}$ requires careful monitoring of eclipse times of minimum. This can only be performed if one has a densely populated light curve.

The data would also permit measurement of the binary eccentricity and semi-major axis with high precision. These properties affect both Equation (2) and the general relativistic contribution discussed in Section 3 (Giménez 1985). Recall that the contribution from the latter must be removed from the total apsidal motion rate to derive the classical contribution given in Equation (1). Detailed radial velocity curves not only provide accurate mass and eccentricity estimates, but may also be used to investigate the inclination of the system. The

[5] Convection, Rotation, & planetary Transients
[6] Wide Angle Search for Planets
[7] Large Synoptic Survey Telescope
[8] Bright Target Explorer

theory presented in Section 3 relies on the assumption that the rotational axes of the two stars be parallel to one another and perpendicular to the orbital plane. It is possible to evaluate this restriction by using the Rossiter-McLaughlin effect in a manner similar to that presented for DI Her (Albrecht et al. 2009). A detailed radial velocity curve may, additionally, betray the presence of a third body. The presence of a tertiary may affect the binary orbit, altering the derived apsidal motion.

One added benefit is that lengthy observations may help to identify—and thus correct for—the impact of star spots and magnetic activity on the eclipse profiles. Star spots have the ability to distort the light curve, which can diminish the accuracy of the derived stellar properties (Windmiller et al. 2010). Removing the effects of spots is critical to obtain not only precise but also accurate stellar properties. The easiest means of obtaining detailed time-series photometry is through space-based satellites, such as CoRoT and *Kepler*. However, long-term ground-based observational efforts are beginning to produce apsidal motion detections (e.g., Zasche 2012), demonstrating that it is feasible to carry out the necessary observations using ground-based telescopes.

Finally, by acquiring a large number of quality spectra, it may be possible to extract the projected rotational velocities ($v \sin i$) and a modest estimate of the chemical composition. Spectroscopic determinations of cool star metallicities is notoriously complicated, but most pre-MS DEBs will likely reside near or in a cluster from which metallicity estimates can be extracted using the higher mass stellar population. In the event there is no known association from which to draw a metallicity, techniques based on low- and medium-resolution spectra are encouraging (see, e.g., Rojas-Ayala et al. 2012). While the validity of such techniques along the pre-MS is unclear, they provide a viable starting point and typically produce metallicities with uncertainties below 0.2 dex, the limit we recommend.

5.2. *Limitations*

The usefulness of $\overline{k_2}$ as an age estimator is limited to the pre-MS, in particular, during the evolutionary phase where the radiative core is rapidly contracting. This typically corresponds to an age between 10 Myr and 100 Myr (see Figure 1). At the 5 – 10 % measurement level, this technique is also restricted to binaries where one of the stars has a mass above $\sim$0.40 $M_\odot$. This restriction ensures the radiative core contraction and relative change in k_2 for the more massive star is rapid enough to dominate the theoretical $\overline{k_2}$ evolution. Reducing the observational uncertainty in $\overline{k_2}$ below 5% enables a more accurate age estimate and would allow for DEBs with lower mass components to be reliably analyzed.

Precise measures of apsidal motion and metallicity are challenging to obtain, but are already feasible and should only improve over time. Instead of observational limitations, the greatest limiting factor for using $\overline{k_2}$ as an age indicator is the circularization of the DEB orbit. Mutual tidal interactions will circularize binary orbits over time (Zahn 1977). Apsidal motion requires an elliptical orbit. If an equal-mass binary is to maintain an elliptical orbit for the duration of its pre-MS contraction, the orbital period must be at least 2.4 days (Zahn 1977). The probability of discovering an elliptical binary decreases with time, but this provides an additional consistency check. The age suggested by $\overline{k_2}$ should not be significantly older than the orbital circularization timescale.

Finally, the age estimate is only as accurate as the stellar models. Verifying that a given stellar model produces the proper mass distribution, hence k_2, may at first seem rather unreasonable. However, at least one known system, with the possibility of a second (KIC 002856960; Lee et al. 2012), is capable of providing validation of the physics incorporated in low-mass stellar evolution models. Carter et al. (2011) have indicated that by the end of the nominal *Kepler* mission, they will know the interior structure constants of KOI-126 B and C with about 1% precision. Interior structure constants known with this precision can place stringent constraints on the equation of state of the stellar plasma (Feiden et al. 2011). The veracity of low-mass models, and therefore the validity of their predicted interior structure constants, may be assessed according to the results from KOI-126 and similar systems.

The authors thanks G. Torres and K. Stassun for insightful conversations, the anonymous referee for helpful comments and suggestions, and Alan Irwin for his work on the open source FreeEOS project. G.A.F. also thanks the Department of Physics and Astronomy at Uppsala University for their gracious hospitality during the completion of the manuscript. G.A.F. acknowledges the support of the William H. Neukom 1964 Institute for Computational Science and the the National Science Foundation (NSF) grant AST-0908345. A.D. received support from the Australian Research Council under grant FL110100012. This research has made use of NASA's Astrophysics Data System.

REFERENCES

Albrecht, S., Reffert, S., Snellen, I. A. G., & Winn, J. N. 2009, Nature, 461, 373
Andersen, J. 1991, A&A Rev., 3, 91
Bahcall, J. N., Basu, S., Pinsonneault, M., & Serenelli, A. M. 2005, ApJ, 618, 1049
Bjork, S. R. & Chaboyer, B. 2006, ApJ, 641, 1102
Carter, J. A., Fabrycky, D. C., Ragozzine, D., et al. 2011, Science, 331, 562
Chaboyer, B., Fenton, W. H., Nelan, J. E., Patnaude, D. J., & Simon F. E. 2001, ApJ, 562, 521
Chaboyer, B. & Kim, Y.-C. 1995, ApJ, 454, 767
Chabrier, G. & Baraffe, I. 2000, ARA&A, 38, 337
Chabrier, G., Gallardo, J., & Baraffe, I. 2007, A&A, 472, L17
Chandrasekhar, S. 1933, MNRAS, 93, 390
Claret, A. 1999, A&A, 350, 56
Claret, A. & Giménez, A. 1993, A&A, 277, 487
Dotter, A., Chaboyer, B., Jevremović, D., et al. 2007, AJ, 134, 376
Dotter, A., Chaboyer, B., Jevremović, D., et al. 2008, ApJS, 178, 89
Feiden, G. A. & Chaboyer, B. 2012a, ApJ, 757, 42
Feiden, G. A. & Chaboyer, B. 2012b, ApJ, 761, 30
Feiden, G. A., Chaboyer, B., & Dotter, A. 2011, ApJ, 740, L25
Ferguson, J. W., Alexander, D. R., Allard, F., et al. 2005. ApJ, 623, 585
Giménez, A. 1985, ApJ, 297, 405
Grevesse, N., & Suaval, A. J. 1998, Space Sci. Rev., 85, 161
Hauschildt, P. H., Allard, F., & Baron, E. 1999a, ApJ, 512, 377
Hauschildt, P. H., Allard, F., Ferguson, J., Baron, E., & Alexander, D. R. 1999b, ApJ, 525, 871
Iglesias, C. A. & Rogers, F. J. 1996, ApJ, 464, 943
Jackson, R. J., Jeffries, R. D., & Maxted, P. F. L. 2009, MNRAS, 339, L89
Kopal, Z., ed. 1978, Astrophysics and Space Science Library, Vol. 68, Dynamics of close binary systems
Lee, J. W., Kim, S.-L., Lee, C.-U., et al. 2013, ApJ, 763, 74
Mathieu, R. D., Baraffe, I., Simon, M., Stassun, K. G., & White, R. 2007 in Protostars & Planets V, 411
McLaughlin, D. B. 1924, ApJ, 60, 22
Michaud, G., Fontaine, G., & Beaudet, G. 1984, ApJ, 282, 206
Morales, J. C., Gallardo, J. J., Ribas, I., et al. 2010, ApJ, 718, 502
Ribas, I. 2006, Ap&SS, 304, 89
Rojas-Ayala, B., Covey, K. R., Muirhead, P. S., & Lloyd, J. P. 2012, ApJ, 748, 93

Rossiter, R. A. 1924, ApJ, 60, 15
Soderblom, D. R. 2010, ARA&A, 48, 581
Stothers, R. 1974, ApJ, 194, 651
Thoul, A. A., Bahcall, J. N., & Loeb, A. 1994, ApJ, 421, 828
Torres, G. 2012, arXiv:1209.1279
Torres, G., Andersen, J., & Giménez, A. 2010, A&A Rev., 18, 67
Windmiller, G., Orosz, J. A., & Etzel, P. B. 2010, ApJ, 712, 1003
Zahn, J.-P. 1977, A&A, 57, 383
Zasche, P. 2012, AcA, 62, 97